Molecular Crystals and Liquid Crystals
Publication details, including instructions for authors and subscription information:
http://www.tandfonline.com/loi/gmcl16

Studies on Mesogenic Disc-like Molecules II. Heat Capacity of Benzenehexa-n-heptanoate from 13 to 393 K

Michio Sorai [a] & Hiroshi Suga [a]
[a] Chemical Thermodynamics Laboratory and Department of Chemistry, Faculty of Science, Osaka University, Toyonaka, Osaka, 560, Japan
Version of record first published: 20 Apr 2011.

To cite this article: Michio Sorai & Hiroshi Suga (1981): Studies on Mesogenic Disc-like Molecules II. Heat Capacity of Benzenehexa-n-heptanoate from 13 to 393 K, Molecular Crystals and Liquid Crystals, 73:1-2, 47-69

To link to this article: http://dx.doi.org/10.1080/00268948108076261

Mol. Cryst. Liq. Cryst., 1981, Vol. 73, pp. 47–69
0026-8941/81/7302–0047 $06.50/0

Printed in the United States of America

Studies on Mesogenic Disc-like Molecules II. Heat Capacity of Benzene-hexa-*n*-heptanoate from 13 to 393 K†

MICHIO SORAI and HIROSHI SUGA

Chemical Thermodynamics Laboratory and Department of Chemistry, Faculty of Science, Osaka University, Toyonaka, Osaka 560, Japan

(*Received March 9, 1981; in final form May 4, 1981*)

The heat capacity of benzene-hexa-*n*-heptanoate, $C_6(OCOC_6H_{13})_6$, with a purity of 99.94 mole per cent has been measured with an adiabatic-type calorimeter in the range from 13 to 393 K. Five phase transitions were found at 129 (Phase IV → III), 222.80 (III → II), 230.81 (II → I), 353.79 (I → "discotic" mesophase) and 359.28 K ("discotic" mesophase → isotropic liquid). The enthalpy and entropy of these transitions were determined. The infrared spectra recorded in the range 4000–30 cm^{-1} remarkably depended on temperature. Characteristic features of the "discotic" mesogen have been elucidated as follows; (i) The mesogen exhibits a rich solid polymorphism accompanied by a large amount of transition entropy. (ii) The heat capacity is smaller in the mesophase than in the adjacent crystalline and isotropic liquid phases. (iii) Short-range order effect of the mesophase still persists in the isotropic liquid phase. (iv) The transition entropy at clearing point is large compared with those of classical liquid crystals and melting entropies of plastic crystals. It is, however, very small portion of the cumulative transition entropy. (v) The infrared spectrum recorded at the mesophase is substantially the same as that at the isotropic liquid. (vi) As far as the transition entropy and the infrared spectra are concerned, paraffinic moieties in the molecule are highly disordered in the mesophase. (vii) A sequential phase transitions in the solid state can be regarded as a successive phase transition concerning the conformational melting of the paraffinic moieties. As a conclusion, the present thermodynamic study suggests that the "discotic" mesophase should be regarded as being situated between typical liquid crystals of rod-like molecules and typical plastic crystals of globular molecules.

1 INTRODUCTION

Since the discovery of a novel mesophase of disc-like molecules by Chandrasekhar *et al.*[1] in 1977 and immediately thereafter by three French groups[2–4] in 1978,

† Contribution No. 17 from Chemical Thermodynamics Laboratory. Part I of this series is Ref. 20.

many efforts[5-23] have been devoted to understanding of this interesting condensed state of matter and the existence of "discotic" mesophase is now well established. An excellent review concerning the development during this period has been given by Billard.[24] However, as to the concept of "discotic" mesophase or, in other words, the characteristic factors which govern the appearance of such a mesophase, unified interpretation based on intermolecular interactions has not necessarily been established yet.

Experimental works hitherto reported are mainly concerned with syntheses of new "discogens", observation of optical textures, miscibility in binary systems, X-ray diffraction analyses and simple thermal analyses (DTA and DSC). We have reported the heat capacity and infrared absorption measurements of benzene-hexa-*n*-hexanoate, $C_6(OCOC_5H_{11})_6$, over a wide temperature range and pointed out that the entropic aspects obtained from thermodynamic study provide an important information about the nature of "discotic" mesophase.[20] Although this compound is not a "discotic" mesogen but belongs to its precursor, similar results were found to be encountered for a true "discotic" mesogen, benzene-hexa-*n*-heptanoate $C_6(OCOC_6H_{13})_6$.[21] The present paper reports a study based on the heat capacity and infrared absorption measurements for this compound.

2 EXPERIMENTAL

Sample preparation

The compound $C_6(OCOC_6H_{13})_6$ was synthesized from inositol (Nakarai Chemicals, Ltd.: Extra Pure Reagent) and *n*-enanthyl chloride (Tokyo Kasei Kogyo Co., Ltd.: Extra Pure Reagent) by the published methods.[25-27] The crude material was recrystallized four times from absolute ethanol to give needle crystals and dried for 24 h in a vacuum. *Anal.* Calcd. for $C_{48}H_{78}O_{12}$: C, 68.06%; H, 9.28%. Found: C, 68.08%; H, 9.34%.

Heat capacity measurements

The heat capacities were measured with an adiabatic-type calorimeter[28] between 13 and 393 K. A calorimeter cell[29] made of gold and platinum contained 17.4339 g (≙ 0.0205798 mol) of the compound and a small amount of helium gas to aid the heat transfer. A platinum resistance thermometer (Leeds & Northrup Co., Ltd.) used in this experiment has been calibrated based on the IPTS-68 temperature scale.

Infrared and far infrared spectroscopy

Spectra in the range 4000–400 cm^{-1} were recorded for Nujol mulls with an Infrared Spectrophotometer Model DS-402G (Japan Spectroscopic Co., Ltd.)

and far infrared spectra in the range 400–30 cm^{-1} with a Far Infrared Spectrophotometer Model FIS-3 (Hitachi, Ltd.) between 90 and 370 K.

Polarizing microscopy

Textures of the phase I and discotic mesophase were observed by a polarizing microscope (Olympus, Model BHA-751-P) equipped with a heating stage (Union Optical Co., Ltd., Model CMS-2). Temperature of the specimen was monitored by a chromel *versus* constantan thermocouple.

3 RESULTS

Prior to the heat capacity measurements, qualitative thermal behavior between 90 and 395 K was examined with a differential thermal analysis (DTA).[30] The DTA curve showed three large endothermic peaks at 230.5, 354.7 and 359.8 K, and a small peak at 224.5 K on a heating run. On the other hand, the three dominant peaks were undercooled down to 358.2, 341.2 and 225.0 K on a cooling run. This fact implies that these three phase transitions are characteristic of a first-order nature. Two highest-temperature transitions correspond to the phase transitions of crystal-to-mesophase and mesophase-to-isotropic liquid, respectively. These temperatures accord well with those reported by Chandrasekhar *et al.*[1,11] The remaining two peaks at 224.5 and 230.5 K newly found here correspond to polymorphism in the solid.

For the heat capacity measurements, careful thermal treatments were made for the specimen with reference to the results of DTA. The sample in a calorimeter cell was once melted and heated up to 362 K. After that, the temperature was very slowly lowered down to *ca.* 60 K in four days. The most stable crystalline phase was thought to be realized through this process. However, heat capacity measurements started from 60 K showed temperature drifts due to heat evolution; indicating that a kind of stabilization phenomenon occurred for the crystal thus cooled. The specimen was then annealed for 21 h in the temperature region 70–80 K. The measurements restarted from 95 K no longer showed the heat evolution effect. But instead, a broad heat capacity anomaly centered at 119 K was observed. We at first thought that this anomaly would arise from a kind of glass-transition phenomenon.[31] As will be described in section 5, however, this anomaly was proved to be caused by a diffuse first-order phase transition. When the specimen was annealed at 70–80 K for 90 h, the heat capacity anomaly was enhanced and its peak was shifted to 129 K. On the other hand, for the specimen rather rapidly cooled from 175 K to 95 K without annealing, the heat capacity anomaly was extremely depressed; an apparent peak being centered at 109 K and its peak height being only 18% of that for the specimen completely annealed.

The results of the calorimetric measurements were evaluated in terms of C_p, the molar heat capacity under a constant pressure. The experimental data are listed in Table I and ploted in Figure 1, where the heat capacities around 129 K correspond to those for the specimen completely annealed and the data obtained for the partially undercooled or quenched samples are not shown. Since three solid-to-solid phase transitions were found at 129, 222.80 and 230.81 K,

TABLE I

Molar heat capacity of C_6 $(OCOC_6H_{13})_6$: Relative molecular mass 847.137

T/K	C_p/J K^{-1} mol^{-1}	T/K	C_p/J K^{-1} mol^{-1}	T/K	C_p/J K^{-1} mol^{-1}
11.479	22.148	124.750	694.13	236.602	1460.8
12.928	30.666	127.497	707.06	239.275	1310.6
14.230	39.320	130.206	716.26	242.750	1249.8
15.457	47.401	132.890	720.18	244.860	1250.3
16.692	55.647	135.553	721.32	250.117	1249.6
17.928	63.888	138.796	727.36	252.560	1256.7
19.382	73.976	141.911	732.53	256.028	1269.8
21.086	86.706	144.763	741.92	260.162	1282.9
22.975	100.83	148.281	752.72	264.258	1304.1
24.979	115.57	152.361	765.99	268.452	1327.2
27.059	131.56	156.036	779.49	272.730	1346.5
29.413	149.62	160.394	793.86	276.260	1372.0
31.896	168.48	164.858	808.79	280.450	1400.2
34.761	190.22	169.427	825.23	284.590	1424.6
38.081	215.08	173.933	841.00	288.877	1451.7
41.314	237.77	176.253	849.28	293.304	1481.8
44.451	259.60	180.740	867.88	297.684	1502.3
48.100	283.32	185.256	886.78	302.022	1528.7
52.103	309.88	189.707	907.51	306.317	1550.0
55.996	335.71	194.093	929.26	313.785	1584.6
59.459	357.58	198.413	952.78	317.556	1606.5
62.194	373.76	202.425	974.59	322.795	1626.5
65.037	391.11	205.917	1000.4	328.720	1652.8
68.354	409.18	210.046	1033.5	331.248	1660.8
72.311	430.95	213.107	1060.6	335.748	1682.4
76.255	451.86	215.127	1084.9	337.487	1684.9
78.372	461.92	217.122	1111.0	340.210	1701.9
80.008	471.02	218.266	1126.2	341.809	1709.4
81.662	479.04	219.087	1144.4	345.365	1723.4
85.377	496.92	220.305	1164.8	347.523	1734.9
88.956	514.12	221.022	1185.5	351.966	2051.7
92.420	529.88	222.303	1205.2	353.629	27391.
96.190	547.91	222.922	1213.9	353.737	180790.
100.650	567.81	224.813	1200.8	353.759	346110.
104.598	585.22	226.709	1199.4	353.773	482340.
107.742	597.45	228.319	1283.9	353.785	386730.
110.290	611.72	229.473	1982.1	353.873	31847.
113.295	627.57	230.327	2692.2	354.885	1663.7
116.241	643.94	231.060	3057.8	355.305	1669.1
119.129	662.75	232.338	2419.9	356.435	1672.5
121.964	678.54	234.286	1764.4	357.669	1683.6

TABLE 1 *continued*

T/K	C_p/J K^{-1} mol^{-1}	T/K	C_p/J K^{-1} mol^{-1}	T/K	C_p/J K^{-1} mol^{-1}
358.756	2101.8	359.284	1611700.	366.721	1869.1
359.237	51484.	359.380	17709.	370.008	1860.2
359.274	482120.	360.051	1882.0	375.165	1854.5
359.279	1100100.	361.760	1877.6	380.326	1851.0
359.282	1679000.	365.162	1870.2	385.481	1849.6
				390.625	1850.5
		Undercooled Mesophase			
347.207	1646.6	348.853	1650.5	350.497	1653.7
				352.547	1661.4
		Partially undercooled Phase III[a]			
97.378	555.53	123.523	680.00	146.285	740.15
100.986	571.89	127.531	687.00	150.644	756.59
105.519	592.86	130.321	694.25	155.104	771.72
110.228	616.05	133.768	699.73	159.245	787.54
114.785	644.56	137.856	711.11	162.850	800.67
119.205	667.83	142.029	724.96	167.277	816.85
				171.796	832.08
		Partially undercooled Phase III[b]			
99.248	564.62	126.092	664.70	153.936	763.47
105.238	590.05	133.199	689.03	160.156	784.92
112.192	617.75	138.896	708.62	165.515	806.06
119.101	641.65	140.300	713.95	171.835	829.87
		147.205	739.65	178.030	855.67

[a] Annealed at 70–80 K for 21 h.
[b] Not annealed.

the crystalline phases bounded by these temperatures will be named as Phases I, II, III and IV in descending direction of temperature. The crystal-to-"discotic" mesophase transition (the so-called melting point) and the mesophase-to-isotropic liquid transition (the clearing point) were found to occur at 353.79 and 359.28 K, respectively.

The time required for thermal equilibration after an energy input was usually 20 min or shorter even in the vicinity of the clearing point, while it was elongated to one hour in the melting region and two hours in the transition region from Phase II to I.

The purity of the sample was determined by a fractional fusion method. Plot of the reciprocal of the fraction melted against the melting temperature gave a straight line, indicating nonexistence of solid-soluble impurities, and the slope yielded a sample purity of 99.94 mole per cent. The triple point of pure material was 353.81 K.

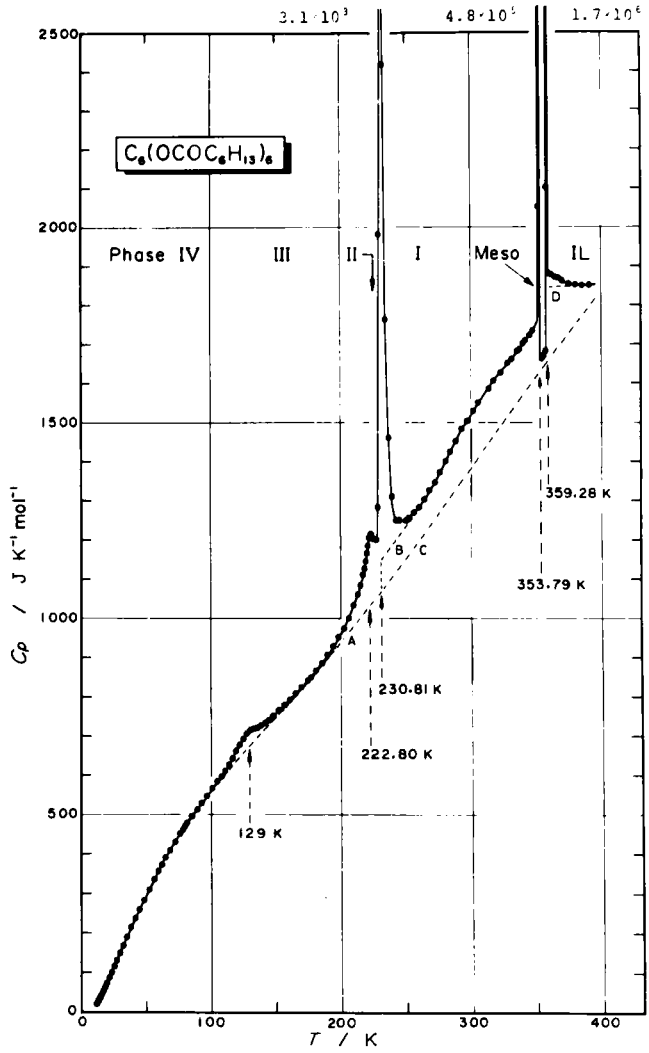

FIGURE 1 Molar heat capacity of $C_6(OCOC_6H_{13})_6$. The "discotic" mesophase and isotropic liquid are abbreviated as Meso and IL, respectively. The broken lines labelled A, B and D represent the normal heat capacities.

The standard thermodynamic functions of $C_6(OCOC_6H_{13})_6$ were calculated from the heat capacity data and the calorimetric enthalpy measurements across the respective phase transitions. Table II contains a listing of values for the heat capacity, C_p°, the entropy, S°, the enthalpy function, $(H^\circ - H_0^\circ)/T$, and the Gibbs energy function, $-(G^\circ - H_0^\circ)/T$, at selected temperatures. The values in parentheses were derived from the effective frequency spectrum, the estimation of which will be described in section 4.

TABLE II

Standard thermodynamic functions for $C_6(OCOC_6H_{13})_6$ in J K^{-1} mol^{-1}

T/K	C_p°	S°	$(H^\circ - H_0^\circ)/T$	$-(G^\circ - H_0^\circ)/T$
5	(2.06)	(0.685)	(0.514)	(0.171)
10	(15.71)	(5.402)	(4.039)	(1.363)
20	78.85	33.931	24.414	9.517
30	154.46	80.169	55.140	25.029
40	227.79	134.75	89.222	45.524
50	296.63	193.06	123.90	69.161
60	360.41	252.86	158.08	94.784
70	418.62	312.87	191.21	121.66
80	471.22	372.26	222.99	149.28
90	518.80	430.56	253.25	177.31
100	564.91	487.58	282.21	205.37
120	667.60	598.95	337.15	261.80
		Phase Transition (IV → III) at 129 K		
140	729.36	707.99	390.12	317.87
160	792.56	809.22	436.28	372.94
180	864.81	906.58	479.72	426.86
200	961.41	1002.4	522.76	479.65
220	1159.7	1101.5	569.82	531.64
		Phase Transition (III → II) at 222.80 K Phase Transition (II → I) at 230.81 K		
240	1297.9	1239.0	654.38	584.59
260	1282.4	1340.1	701.00	639.07
280	1397.2	1438.8	746.36	692.42
298.15	1505.2	1530.0	789.38	740.62
300	1516.4	1539.3	793.79	745.55
320	1615.8	1640.5	842.16	798.32
340	1700.6	1740.9	890.16	850.78
		Phase Transition (I → Mesophase) at 353.79 K Phase Transition (Mesophase → Liquid) at 359.28 K		
360	1882.1	1989.5	1084.6	904.88
380	1851.2	2090.2	1125.6	964.60
390	1850.4	2138.2	1144.1	994.09

Infrared spectra recorded at all phases are reproduced in Figures 2, 3, and 4. As in the case of $C_6(OCOC_5H_{11})_6$,[20] temperature dependence of the spectra was remarkable. Drastic changes were observed on going from Phase II to I and from Phase I to the mesophase; indicating that the crystal structures and the molecular arrangements are quite different among these phases. On the other hand, the spectra of the mesophase were substantially the same as those of the isotropic liquid phase. This fact strongly suggests that the molecular motions in the mesophase are as random as in the isotropic liquid phase.

The optical observation by a polarizing microscope equipped with a heating stage showed characteristic textures for Phase I and the mesophase. When the

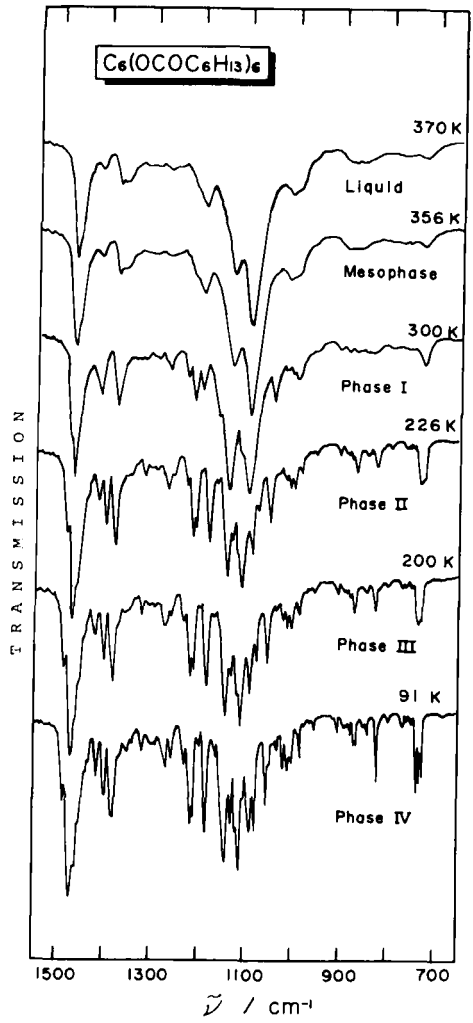

FIGURE 2 Infrared spectra of $C_6(OCOC_6H_{13})_6$.

sample was cooled from isotropic liquid to the mesophase, a variant of the focal conic texture with spherulitic domains appeared (Figure 5(a)). Under a high magnification of 400×, fan-shaped textures were clearly recognized (Figure 5(b)). This texture is similar to those observed previously.[11,23] Although the texture is rather smeared, texture domains of circular bending showing oblique extinction brushes[23] are also recognized in Figure 5(b). On going from the mesophase to Phase I, the optical texture showed quite different pattern (Figure 5(c)).

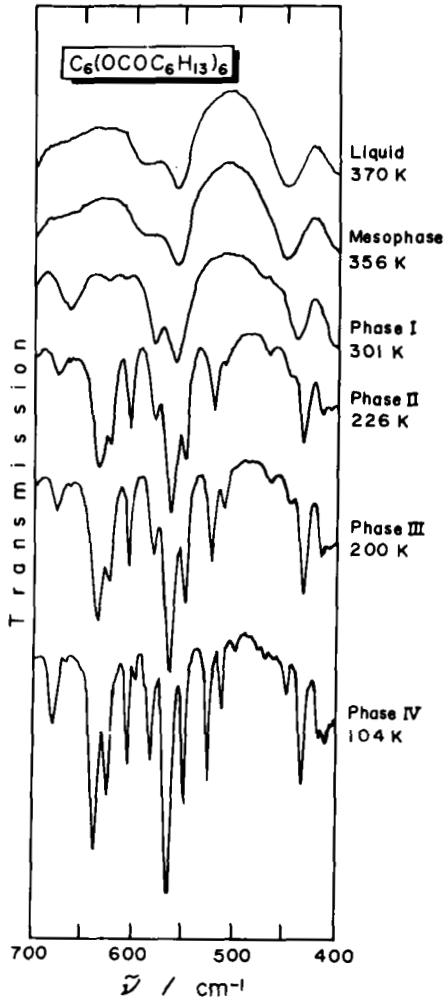

FIGURE 3 Infrared spectra of $C_6(OCOC_6H_{13})_6$.

4 ENTHALPY AND ENTROPY OF PHASE TRANSITION

To separate the excess heat capacities due to the phase transitions from the experimental values, we must estimate appropriate "normal" heat capacities. As pointed out in section 3, the phase transitions at 230.81, 353.79 and 359.28 K are of a first-order and hence may involve a volume change. In such a case the normal heat capacity is expected to bring about a discontinuity at a transition point. Normal heat capacities below 230.81 K, corresponding to those for Phases II, III and IV, were estimated according to an effective frequency spec-

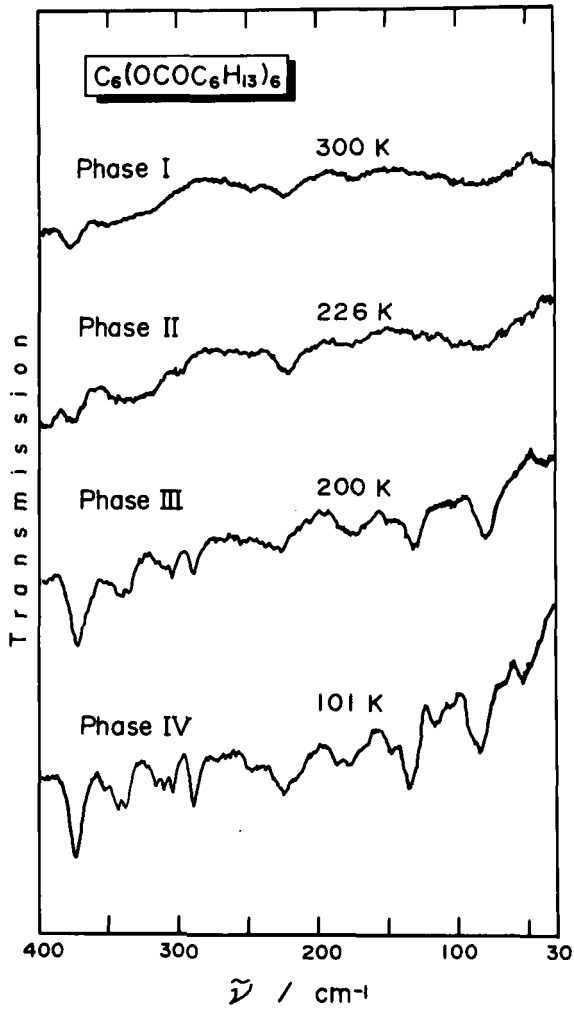

FIGURE 4 Far infrared spectra of $C_6(OCOC_6H_{13})_6$.

trum method.[32] This method is to reproduce the experimental heat capacity by using an effective frequency spectrum consisting of continuous and discrete distributions of lattice vibration frequencies. For this estimation, we used 40 C_p values between 11.5 and 172 K except for the region from 97 to 138 K, where the heat capacity anomaly due to the phase transition is apparent, and the vibrational frequencies of 39 modes (372 degrees of freedom) obtained from the infrared spectra in the range from 2950 to 669 cm^{-1}. A "best" fit was obtained for a continuous spectrum consisting of two Debye-type and three

constant distributions; $G(\tilde{\nu}) = 0.2269 \times 10^{-3}\tilde{\nu}^2 (0 - 60\,\mathrm{cm}^{-1})$, $G(\tilde{\nu}) = 0.6666 \times 10^{-4}\tilde{\nu}^2 (60 - 100\,\mathrm{cm}^{-1})$, $G(\tilde{\nu}) = 0.3270 (100 - 300\,\mathrm{cm}^{-1})$, $G(\tilde{\nu}) = 0.3227 \times 10^{-1} (300 - 500\,\mathrm{cm}^{-1})$ and $G(\tilde{\nu}) = 0.2027 (500 - 700\,\mathrm{cm}^{-1})$.† The effective spectrum thus obtained was able to reproduce the experimental C_p values in this temperature region within $\pm 0.603\,\mathrm{J\,K^{-1}\,mol^{-1}}$. The normal heat capacities calculated from this spectrum is shown by the broken line (A) in Figure 1. The broken curve (C) above 230.81 K corresponds to the heat capacities due to this spectrum. The normal heat capacity of the low temperature region of Phase I (the broken curve (B)) was estimated by simply lifting the curve (C) by $83\,\mathrm{J\,K^{-1}\,mol^{-1}}$. In the isotropic liquid phase, the normal heat capacity was regarded as being represented by a straight line connecting two highest-temperature C_p points at 385.481 and 390.625 K (the broken line (D)). The enthalpy and entropy of phase transitions were determined as being the excess contributions beyond these normal heat capacities. For these calculations, the results of the calorimetric enthalpy measurements across the respective phase transitions were also taken into account. The numerical data concerning the thermodynamic quantities due to the phase transitions are summarized in Table III.

Figure 6 represents the temperature dependence of the entropy acquisition due to the phase transitions. In spite of the fact that the present molecule has six excess methylene groups compared with $C_6(OCOC_5H_{11})_6$, the cumulative entropy of all the phase transitions ($209.91\,\mathrm{J\,K^{-1}\,mol^{-1}}$) is much smaller than $286.32\,\mathrm{J\,K^{-1}\,mol^{-1}}$ found for the latter.[20] In the case of $C_6(OCOC_5H_{11})_6$, the successive phase transitions were well interpreted in terms of the conformational melting of the paraffinic chains progressing from the periphery of a molecule into its inside each time a phase transition takes place.[20] If this picture could directly be applied for the present case, the cumulative entropy should be about $62\,\mathrm{J\,K^{-1}\,mol^{-1}}$ (the entropy gain per six methylene groups[20]) higher than the entropy of $C_6(OCOC_5H_{11})_6$. In this regard, the reversion of the cumulative entropies elucidated for the present homologous series seems to be quite curious. As shown in Figure 7, however, the standard entropy of the present compound exceeded that of $C_6(OCOC_5H_{11})_6$ over the whole temperature region investigated here. The entropy difference between them at, say, 390 K amounted to *ca.* $240\,\mathrm{J\,K^{-1}\,mol^{-1}}$, which is about four times larger than the entropy gain expected for six methylene groups. Moreover, the heat capacity difference at 390 K was *ca.* $240\,\mathrm{J\,K^{-1}\,mol^{-1}}$. This value also exceeds the value of $189\,\mathrm{J\,K^{-1}\,mol^{-1}}$ expected for six methylene groups.[33] These facts obviously suggest that a large amount of the conformational melting of the paraffinic chains in $C_6(OCOC_6H_{13})_6$ may proceed without accompanying phase transitions.

†The two Debye-type distributions in Ref. 20 should be read as $G(\tilde{\nu}) = 0.1517 \times 10^{-3}\tilde{\nu}^2$ $(0 - 45\,\mathrm{cm}^{-1})$ and $G(\tilde{\nu}) = 0.8236 \times 10^{-4}\tilde{\nu}^2\,(45 - 100\,\mathrm{cm}^{-1})$.

(a)

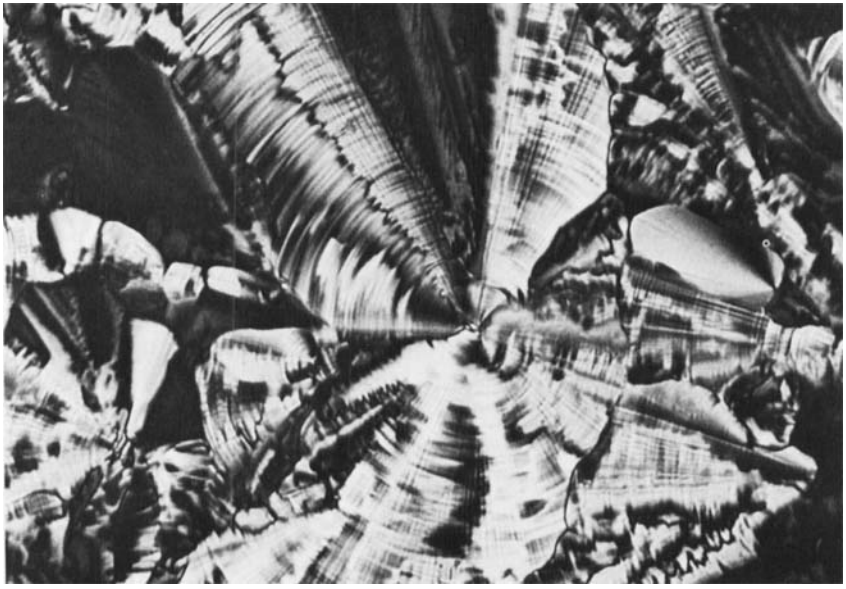

(b)

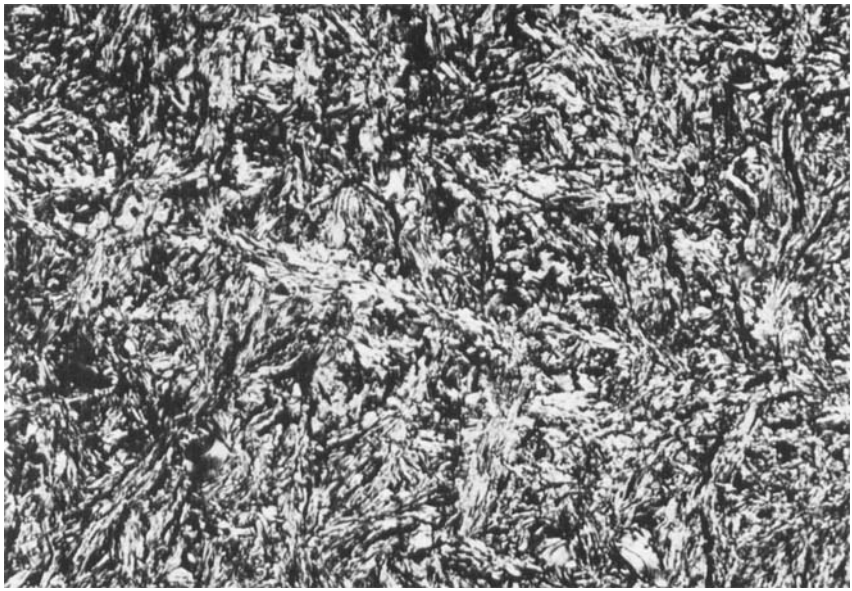

(c)

FIGURE 5 Optical textures of the columnar mesophase (a and b) and Phase I (c) of $C_6(OCOC_6H_{13})_6$. Magnification: 100× for (a) and (c), and 400× for (b).

The entropy change of 59.93 J K^{-1} mol^{-1} due to the transition from the mesophase to isotropic liquid is considerably large compared with those of usual liquid crystals. The transition entropies obtained for nematic and cholesteric mesogens are very small (generally less than several J K^{-1} mol^{-1}), whereas those for smectic are somewhat large. For instance, Arnold *et al.*[34] has reported an entropy change of about 20 J K^{-1} mol^{-1} for a smectic-A and an exceptionally large value of 58 J K^{-1} mol^{-1} for a smectic-C liquid crystal. But in general, the entropy changes encountered for smectic-C mesogens[35-37] are in the range from 13 to 33 J K^{-1} mol^{-1}. However, it should be noticed here that the present molecule has six paraffinic chains in contrast to two paraffinic chains of usual rod-like liquid crystals. If this fact is taken into account, comparison of the transition entropy should be made by using one third of the value obtained for the present "discotic" mesogen, i.e., *ca.* 20 J K^{-1} mol^{-1}. As far as this value is concerned, the present "discotic" mesophase bears a resemblance to usual smectic mesogens.

On the other hand, the transition entropy of 59.93 J K^{-1} mol^{-1} is not so small compared with the entropy change of 90.86 J K^{-1} mol^{-1} found for the Phase I-to-liquid transition for $C_6(OCOC_5H_{11})_6$.[20] This fact does not necessarily imply that the degree of configurational disorder of the present molecule is

TABLE III

Enthalpy and entropy of phase transitions in $C_6(OCOC_6H_{13})_6$

Transition	T_c/K	ΔH/kJ mol^{-1}	ΔS/J K^{-1} mol^{-1}
Phase IV → Phase III	129	1.12	8.46
Phase III → Phase II	222.80	11.5	50.44
Phase II → Phase I	230.81		
Phase I → Mesophase	353.79	32.21	91.08
Mesophase → Liquid	359.28	21.54	59.93
			total 209.91

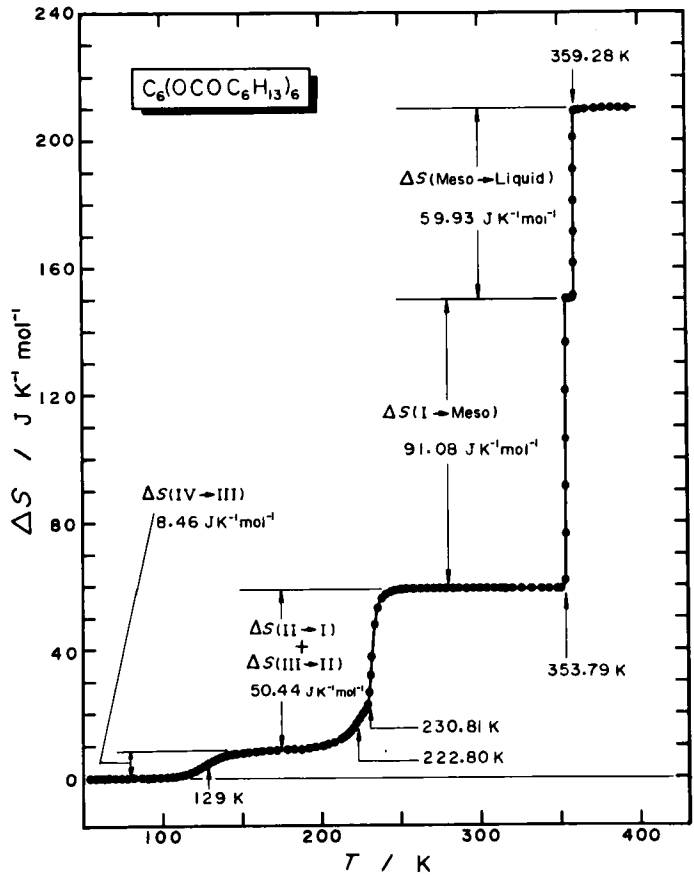

FIGURE 6 The temperature dependence of the entropy acquisition due to the phase transitions found for $C_6(OCOC_6H_{13})_6$.

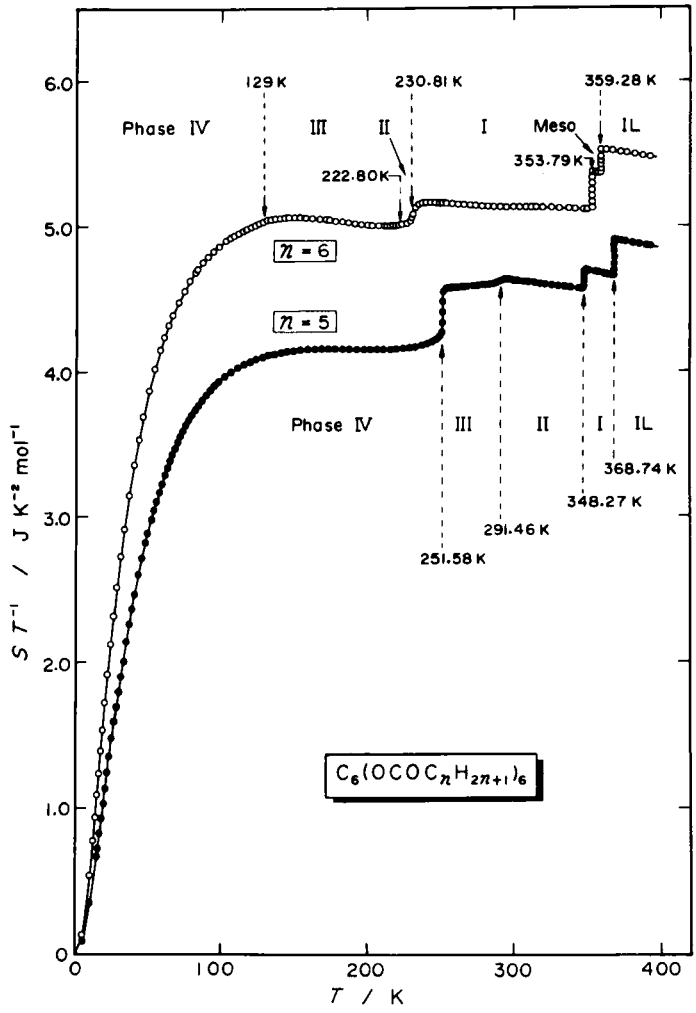

FIGURE 7 Temperature dependence of the molar entropy divided by temperature for $C_6(OCOC_6H_{13})_6$ and $C_6(OCOC_5H_{11})_6$.[20]

low in the mesophase but suggests that the highest-temperature solid phase (Phase I) of $C_6(OCOC_5H_{11})_6$ is regarded as being a highly disordered crystalline phase concerning conformations of the paraffinic chains. At any rate, it is quite interesting that, although the highest-temperature phase adjacent to isotropic liquid phase can be characterized as a highly disordered condensed state for both $C_6(OCOC_5H_{11})_6$ and $C_6(OCOC_6H_{13})_6$, the phase of the latter belongs to a mesomorphic state while the former remains to be a crystalline state.

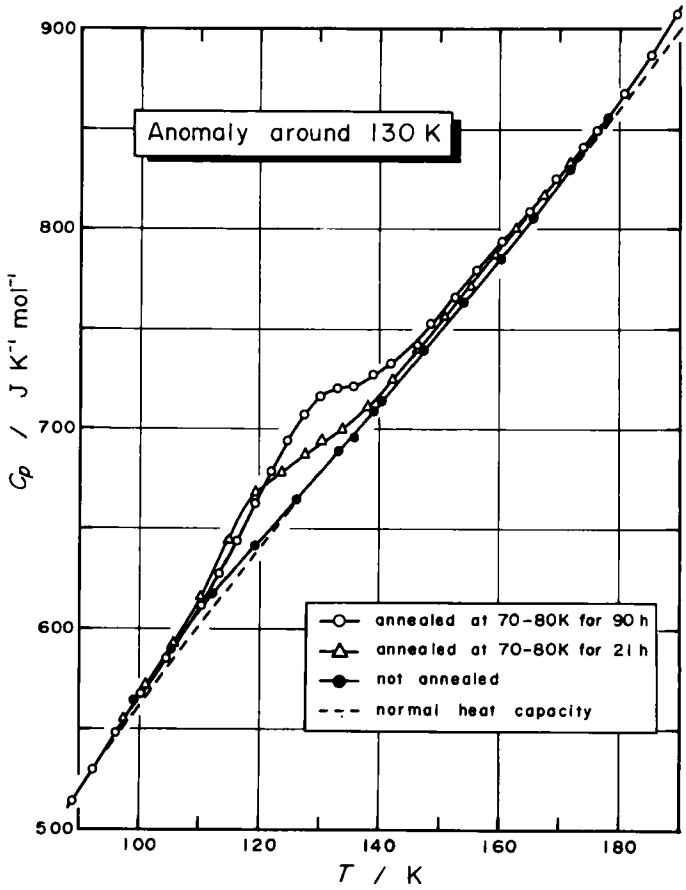

FIGURE 8 The heat capacity anomaly around 130 K.

5 HEAT CAPACITY ANOMALY AROUND 130 K

As described in section 3, the heat capacity anomaly around 130 K remarkably depended on thermal history of the specimen. The results of three series of measurements are plotted in Figure 8 in an enlarged scale. To illustrate the anomalies more clearly, the excess parts, ΔC_p, beyond the normal heat capacity curve have been depicted in Figure 9. Longer annealing of the specimen at 70–80 K brought about higher peak height of ΔC_p and shifted the center of peak to higher temperature side. Since the heat capacity measurements for the sample annealed at 70–80 K for 90 h showed no temperature drifts due to stabilization, the heat capacity curves shown by open circles in Figures 8 and 9 seem to reflect the true heat capacity of the present compound in a completely

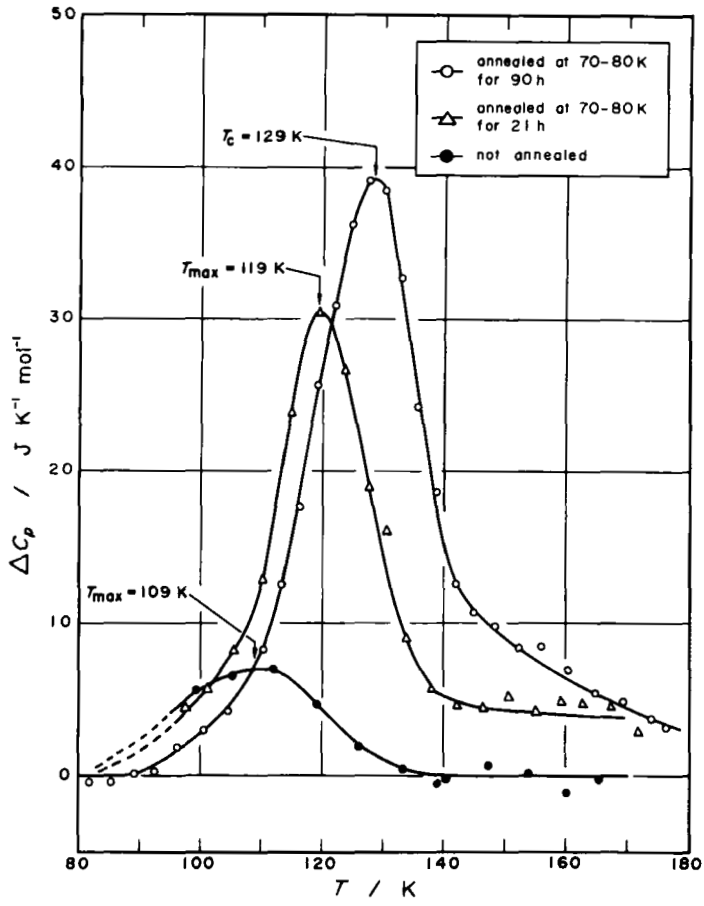

FIGURE 9 Excess heat capacities around 130 K beyond the normal heat capacity curve.

thermal equilibrium. Therefore, the peak temperature of 129 K can be regarded as a kind of critical temperature, T_C, and is distinguished from T_{max} of other series of measurements, at which ΔC_p gives an apparent maximum value.

As mentioned briefly in section 3, we at first imagined that this anomaly would be caused by a kind of glass-transition phenomenon.[31] However, if this is the case, the temperature drift would be exothermic below a glass-transition point, T_g, and become endothermic above T_g. The present measurements showed only exothermic drifts in the temperature region from 60 to 95 K; the largest drift being observed in the range 70–80 K. Moreover, additional evidence for non-glass transition phenomenon has been provided by the anneal-

ing experiments. When a glassy material is annealed below T_g, a stepwise shaped heat capacity anomaly is usually shifted to low temperature side. The annealing effect for the present system shifted the peak to the reverse direction, namely high temperature side. In view of these experimental facts, the present heat capacity anomaly can be concluded to be caused not by a glass transition phenomenon but by a diffuse first-order phase transition, in which a hysteresis loop may spread over a wide temperature region, say, from 60 to 180 K and a usual rectangular loop may be deformed to a parallelogram.

Temperature dependence of the excess enthalpy due to the anomaly around 130 K is shown in Figure 10, where the zero-point of enthalpy has been taken at 190 K. The transition enthalpy estimated for the perfect transition amounted to 1.12 kJ mol^{-1} and the entropy was 8.46 J K^{-1} mol^{-1}.

6 NATURE OF MESOMORPHIC PHASE

"Discotic" mesophase was thought at the early stage of its investigations to contradict the accepted picture of classical liquid crystals in the following four

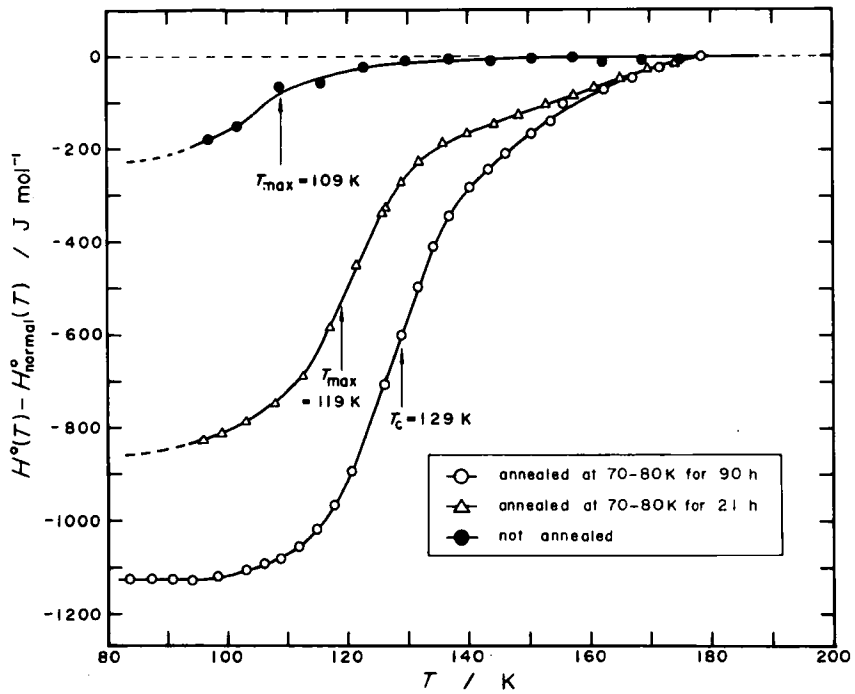

FIGURE 10 Temperature dependence of the excess enthalpy due to the anomaly around 130 K. The zero point of enthalpy has been taken at 190 K.

points. (i) The molecules have two-dimensional or disc-like molecular structure, as opposed to one-dimensional rod-like (usual liquid crystal) or three-dimensional globular (plastic crystal) structures. (ii) Since the disc-like molecules have high symmetries such as a sixfold (6/mmm)[1,11] or a threefold (3/mm, 3)[2-4,9,10] symmetry, the molecules seem to have no net permanent electric dipole moment, which is not a dominant intermolecular interaction to realize a liquid crystalline state but seems to be at least a necessary condition. (iii) The "discotic" mesophases are known to be of optical uniaxis with an optically negative sign.[3] Nematic and smectic mesogens usually exhibit uniaxially (or biaxially for some of smectic sub-classes) positive optical properties, while cholesteric mesogen shows uniaxial negative sign.[38] It is not likely, however, that "discotic" mesogens are optically active and belong to cholesteric mesophase. (iv) The X-ray diffraction patterns[1,5,11] prove that the disc-like molecules are arranged in hexagonal columns in the mesomorphic phases.

However, many counterevidences against each item have been thereafter reported. As to the criterion (i), recent X-ray diffraction study[12] revealed that the molecular configuration of triphenylene esters belonging to the typical disc-like molecules, though they are no "discotic" mesogens, is not disc-like in a crystalline state; six ester chains are alternatively situated up and down the triphenylene core-plane and molecules are associated in pairs. Since the stability of a pair formed is very high, such pairs are supposed to persist in the mesophase and probably to some extent in the liquid phase.[13] The molecular structure of diisobutylsilanediol, which is thought to be a precursor of columnar mesogen,[39,40] is obviously non-planar even if a dimer is formed by hydrogen-bonding. Moreover, we obtained additional evidence for non-planarity of "discotic" molecules from calorimetric measurements;[20,21] judging from entropy, the "discotic" molecules are not so planar in the mesophase but are even globular because conformational melting of flexible paraffinic chains proceeds to a great extent.

In regard to the item (ii), those "discotic" mesogens the molecular structures of which are characterized by lower symmetries (2mm, 2/m, mmm) were synthesized.[14,16,18] Among them, dissymmetric hexasubstituted triphenylenes[14] can principally have permanent electric dipole moment as a whole molecule. Moreover, among usual rod-like liquid crystal compounds, symmetric tolanes[41] and dithiene complexes including metal atoms[42,43] have a twofold symmetry and hence no permanent electric dipole moment.

As concerns the item (iii), some of the Ringsdorf polymers have recently been found to be a negative uniaxial mesogen,[44] though they are no "discotic" mesogens.

Finally as to (iv), many molecular arrangements in "discotic" mesophases other than the hexagonal columnar packing have been proved.[8,15,19,22,45-47] As in the case of classical liquid crystals, polymorphism has now been known to

exist in "discotic" mesogens.[7,8,10,15,16,19,22,45–47] Although there remain possibilities that some other "discotic" mesophases would be discovered in future, Destrade *et al.*[15,19] have classified the existing "discotic" mesophases as D_{ho}, $D_t(D_t^*)$, D_{hd}, D_{rd} and $N_D(N_D^*)$ according to different stacking and packing of molecules, while Billard[24] has adopted different notations.

In view of these present status reviewed above, a simple question may arise whether or not fundamental differences do exist between "discotic" mesophases and classical liquid crystals. Destrade *et al.*[15,45] have suggested that the important difference between them is the director of mesogen; for disc-like molecules the director should be perpendicular to a molecular plane while for classical rod-like molecules it is parallel to a molecular axis. Although this suggestion is surely a discerning idea, other essential differences beyond a problem of the director seem to be hidden. In fact, even if the subject is restricted to the present thermodynamic study, we can easily point out a few new aspects characteristic of the "discotic" mesophase. We shall discuss these aspects by comparing with classical liquid crystals and, when necessary, with plastic crystals.

One of the characteristic features is a rich solid polymorphism. Strictly speaking, the important thing which should be emphasized is not the number of solid polymorphism but a large amount of entropy acquired through the solid-solid transitions. This entropy for the present compound amounted to 58.90 J K^{-1} mol^{-1}, corresponding to as much entropy as sixty-five per cent of the melting entropy of 91.08 J K^{-1} mol^{-1} (see Table III and Figure 6). In the case of $C_6(OCOC_7H_{15})_6$,[48] the entropy due to a solid transition (164.01 J K^{-1} mol^{-1}) far exceeds the melting entropy of 129.81 J K^{-1} mol^{-1}. Except for some of *p-n*-alkoxy-benzoic-acids,[35] solid-solid transitions have scarcely been known for those classical liquid crystals for which thermal property of solid phase has been investigated down to sufficiently low temperatures. Contrary to this, plastic crystals exhibit dominant solid-solid phase transition(s), the entropy of which is in general comparable with or much larger than the melting entropy. In this regard, "discotic" mesogens can be regarded as bearing the aspects characteristic of plastic crystals[49] together with the natures of liquid crystals.

In a previous paper,[20] we have elucidated that the rich solid polymorphism is caused by the successive conformational melting of the paraffinic chains bonded to a benzene core. The existence of such paraffinic chains and their random motion in a solid state seem to play an important role for the appearance of a "discotic" mesophase. In fact, polycyclic aromatics having no paraffinic chains such as coronene, ovalene, decacyclene, etc. exhibit neither "discotic" mesophase nor rich solid polymorphism,[50] although their molecular structures are much more disc-like than the existing discotic mesogens.

Another remarkable feature is that the heat capacity of the mesomorphic phase is much smaller than those of the adjacent crystalline and isotropic liq-

uid phases. As seen in Figure 1, the heat capacity is lowered about 97 J K^{-1} mol^{-1} on going from Phase I to the mesomorphic phase while it is raised about 158 J K^{-1} mol^{-1} by the mesophase-to-liquid transition. In view of the fact that classical rod-like liquid crystals have always shown larger heat capacity in their mesophases than in the adjacent solid and liquid phases,[29,34,51-54] this feature seems to be one of the essential natures of the "discotic" mesophase. A possible origin responsible for the lower heat capacity in the mesophase than in the solid phase may arise from excitations in rotational-vibration modes of the paraffinic moieties. One-dimensional rotator is known to exhibit its heat capacity maximum of the order of the gas constant (R) in the temperature region where the thermal energy is comparable with its potential barrier, while the heat capacity approaches to $R/2$ in the limit of free-rotator.[55] As shown in Figures 2 and 3, the infrared spectra of the mesophase are substantially the same as those of the liquid, indicating highly disordered nature of the paraffinic chains even in the mesophase. On the other hand, the low heat capacity of the mesophase compared with the isotropic liquid may be attributed to both excitations of translational modes and volumetric effect due to thermal expansion at the clearing point.

It should be also remarked here that the "discotic" mesogen exhibits a short-range order effect still persisting in the isotropic liquid state, which appears as the heat capacity tail above the clearing point (see Figure 1). This type of short-range order was also observed for a mesogenic homologue, $C_6(OCOC_7H_{15})_6$.[48] In contrast to this, a non-mesogenic homologue, $C_6(OCOC_5H_{11})_6$, did not show such an effect;[20] the heat capacity in the liquid phase was represented by a straight line almost parallel to the axis of abscissas similar to the broken line labelled D in Figure 1.

Although it is still difficult at the present stage to point out the fundamental character of the "discotic" mesophases to be distinguished from classical liquid crystals, we can conclude that the present thermodynamic study suggests that the "discotic" mesophases should be regarded as being situated between typical liquid crystals of rod-like molecules and typical plastic crystals of globular molecules. Many workers have so far studied "discotic" mesogens only in narrow temperature regions in which they exhibit the mesomorphic phases. However, the present results clearly showed importance of the study over a wide temperature region, because the mesophase is a phenomenon appearing as one stage of the successive phase transition due to the conformational meltings and its properties are closely reflected by the integrated history in the crystalline state.

Acknowledgments

One of the authors (M.S.) expresses his sincere thanks to Professor J. Billard and Dr. C. Destrade for their comments on the counterevidences against the early images about the discotic meso-

gens. The authors acknowledge Itoh Science Foundation for supplying them a polarizing microscope equipped with a heating stage. The infrared spectra were recorded by Messrs. S. Ishikawa and T. Yamamoto, to whom thanks are due.

References

1. S. Chandrasekhar, B. K. Sadashiva and K. A. Suresh, *Pramana,* **9,** 471 (1977).
2. N. H. Tinh, J. C. Dubois, J. Malthete and C. Destrade, *C. R. Acad. Sci. Paris,* **C286,** 463 (1978).
3. J. Billard, J. C. Dubois, N. H. Tinh and A. Zann, *Nouv. J. Chim.,* **2,** 535 (1978).
4. J. C. Dubois, *Ann. Phys.,* **3,** 131 (1978).
5. A. M. Levelut, *J. Phys.,* **40,** L-81 (1979).
6. J. Billard and B. K. Sadashiva, *Pramana,* **13,** 309 (1979).
7. C. Destrade, M. C. Mondon-Bernaud and N. H. Tinh, *Mol. Cryst. Liq. Cryst.,* **49,** L-169 (1979).
8. N. H. Tinh, C. Destrade and H. Gasparoux, *Phys. Lett.,* **72A,** 251 (1979).
9. A. Beguin, J. Billard, J. C. Dubois, N. H. Tinh and A. Zann, *J. Phys.,* **40,** C3-15 (1979).
10. C. Destrade, M. C. Mondon and J. Malthete, *J. Phys.,* **40,** C3-17 (1979).
11. S. Chandrasekhar, B. K. Sadashiva, K. A. Suresh, N. V. Madhusudana, S. Kumar, R. Shashidhar and G. Venkatesh, *J. Phys.,* **40,** C3-120 (1979).
12. M. Cotrait, P. Marsau, C. Destrade and J. Malthete, *J. Phys.,* **40,** L-519 (1979).
13. M. Pesquer, M. Cotrait, P. Marsau and V. Volpilhac, *J. Phys.,* **41,** 1039 (1980).
14. N. H. Tinh, M. C. Bernaud, G. Sigaud and C. Destrade, *Mol. Cryst. Liq. Cryst.,* **65,** 307 (1981).
15. C. Destrade, N. H. Tinh, J. Malthete and J. Jacques, *Phys. Lett.,* **79A,** 189 (1980).
16. A. Quequiner, A. Zann, J. C. Dubois and J. Billard, *Liquid Crystals* edited by S. Chandrasekhar (Heyden and Son, London, 1980), p. 35.
17. J. W. Goodby, P. S. Robinson, B. K. Teo and P. E. Cladis, *Mol. Cryst. Liq. Cryst.,* **56,** L-303 (1980).
18. R. Fugnitto, H. Strzelecka, A. Zann, J. C. Dubois and J. Billard, *J. Chem. Soc. Chem. Commun.,* 271 (1980).
19. C. Destrade, J. Malthete, N. H. Tinh and H. Gasparoux, *Phys. Lett.,* **78A,** 82 (1980).
20. M. Sorai, K. Tsuji, H. Suga and S. Seki, *Mol. Cryst. Liq. Cryst.,* **59,** 33 (1980).
21. M. Sorai, K. Tsuji, H. Suga and S. Seki, *Liquid Crystals* edited by S. Chandrasekhar (Heyden and Son, London, 1980), p. 41.
22. A. M. Levelut, C. Destrade, N. H. Tinh, H. Gasparoux and J. Malthete, International Conference on Liquid Crystals, Bangalore (1979).
23. F. C. Frank and S. Chandrasekhar, *J. Phys.,* **41,** 1285 (1980).
24. J. Billard, *Liquid Crystals on One- and Two-Dimensional Order* edited by W. Helfrich and G. Heppke (Springer, Berlin, 1980), p. 383.
25. F. A. Hoglan and E. Bartow, *J. Am. Chem. Soc.,* **62,** 2397 (1940).
26. I. E. Neifert and E. Bartow, *J. Am. Chem. Soc.,* **65,** 1770 (1943).
27. *Organic Syntheses,* Coll. Vol. 5, 595 and 1011 (1973).
28. M. Yoshikawa, M. Sorai, H. Suga and S. Seki, to be published.
29. K. Tsuji, M. Sorai, H. Suga and S. Seki, *Mol. Cryst. Liq. Cryst.,* **55,** 71 (1979).
30. H. Suga, H. Chihara and S. Seki, *Nippon Kagaku Zasshi,* **82,** 24 (1961).
31. H. Suga and S. Seki, *J. Non-Cryst. Solids,* **16,** 171 (1974).
32. M. Sorai and S. Seki, *J. Phys. Soc. Japan,* **32,** 382 (1972).
33. H. L. Finke, M. E. Gross, G. Waddington and H. M. Huffman, *J. Am. Chem. Soc.,* **76,** 333 (1954).
34. H. Arnold, J. Jacobs and O. Sonntag, *Z. Phys. Chem. (Leipzig),* **240,** 177 (1969).
35. A. J. Herbert, *Trans. Faraday Soc.,* **63,** 555 (1967).
36. T. Hatakeyama and M. Ikeda, *Mol. Cryst. Liq. Cryst.,* **45,** 275 (1978).
37. M. E. Neubert, J. P. Ferrata and R. E. Carpenter, *Mol. Cryst. Liq. Cryst.,* **53,** 229 (1979).
38. G. W. Smith, *Advances in Liquid Crystals,* Vol. 1, edited by G. H. Brown (Academic Press, New York, 1975), p. 189.

39. C. Eaborn and N. H. Hartshorne, *J. Chem. Soc.*, 549 (1955).
40. J. D. Bunning, J. W. Goodby, G. W. Gray and J. E. Lydon, *Liquid Crystals of One- and Two-Dimensional Order*, edited by W. Helfrich and G. Heppke (Springer, Berlin, 1980), p. 397.
41. M. J. Malthete, M. Leclercq, J. Gabard, J. Billard and J. Jacques, *C. R. Acad. Sci. Paris*, **C273**, 265 (1971).
42. A. M. Giroud and U. T. M. Westerhoff, *Mol. Cryst. Liq. Cryst.*, **41**, L-11 (1977).
43. U. T. M. Westerhoff, A. Nazzal, R. J. Cox and A. M. Giroud, *Mol. Cryst. Liq. Cryst.*, **56**, L-249 (1980).
44. H. Kelker and U. G. Wirzing, *Mol. Cryst. Liq. Cryst.*, **49**, L-175 (1979).
45. C. Destrade, M. C. Mondon-Bernaud, H. Gasparoux, A. M. Levelut and N. H. Tinh, *Liquid Crystals*, edited by S. Chandrasekhar (Heydon and Son, London, 1980), p. 29.
46. C. Destrade, A. M. Levelut, M. C. Bernaud and N. H. Tinh, the 8th International Liquid Crystal Conference, Kyoto (1980).
47. J. Billard, J. C. Dubois, C. Vaucher and A. M. Levelut, *Mol. Cryst. Liq. Cryst.*, **66**, 115 (1981).
48. M. Sorai, K. Tsuji, H. Suga and S. Seki, the 8th International Liquid Crystal Conference, Kyoto (1980).
49. J. Timmermans, *J. Chim. Phys.*, **35**, 331 (1938).
50. G. W. Smith, *Mol. Cryst. Liq. Cryst.*, **64**, L-15 (1980).
51. H. Arnold and P. Roediger, *Z. Phys. Chem. (Leipzig)*, **239**, 283 (1968).
52. M. Sorai and S. Seki, *Mol. Cryst. Liq. Cryst.*, **23**, 299 (1973).
53. M. Sorai, T. Nakamura and S. Seki, *Bull. Chem. Soc. Japan*, **47**, 2192 (1974).
54. K. Tsuji, M. Sorai, H. Suga and S. Seki, *Mol. Cryst. Liq. Cryst.*, **41**, L-81 (1977).
55. K. S. Pitzer and W. D. Gwinn, *J. Chem. Phys.*, **10**, 428 (1942).